Chaos, Solitons and Fractals 137 (2020) 109813

Contents lists available at ScienceDirect

Chaos, Solitons and Fractals

Nonlinear Science, and Nonequilibrium and Complex Phenomena

journal homepage: www.elsevier.com/locate/chaos

Dynamics in the transition case invertible/non-invertible in a 2D Piecewise Linear Map

Laura Gardini [a], Wirot Tikjha [b,c,*]

[a] Department DESP, University of Urbino, Italy
[b] Faculty of Science and Technology, Pibulsongkram Rajabhat University, 65000, Thailand
[c] Centre of Excellence in Mathematics, PERDO, CHE, Thailand

ARTICLE INFO

Article history:
Received 12 December 2019
Revised 8 April 2020
Accepted 9 April 2020

2010 MSC:
35B32
37G35

Keywords:
Two-dimensional piecewise linear maps
non-invertibility
first return map
infinitely many inverses
maps of type $Z_0 - Z_1 - Z_\infty$

ABSTRACT

We consider the dynamics of a family of two-dimensional piecewise linear maps at the transition between the invertible and non-invertible cases. This leads to a degeneracy consisting of a half plane which is mapped onto a straight line, the critical line LC. In these regimes the ω-limit set of the trajectories must be on the images of some segment of LC. Thus, the first return map along this line can help in defining the global dynamic behavior of the two-dimensional map. In other cases, the first return map helps in determining some attracting sets, although not the unique attractors of the two-dimensional map.

1. Introduction

The interest in the dynamic behaviors and bifurcations occurring in piecewise smooth two-dimensional maps has been constantly growing in the last two decades, mainly due to the relevant applications of these maps in the applied context. Often these maps arise as Poincaré return maps of dynamical systems in continuous time that are subject to impacts or discrete switching surfaces, but also as true piecewise smooth systems in discrete time which represent applications to economics and social siences. Systems of the first kind can be found, for example, in [1–5]. Systems of the second kind can be found, for example, in [6–10].

The existence of a set crossing which the map changes definition leads to new kind of bifurcations with respect to those which may occur in smooth systems. That is, when an invariant set, typically the periodic point of a cycle, merges with the border of definition, then a drasting change may occur, as evidenced in [11,12], where the term *border collision bifurcations* has been introduced for the first time, and thereafter used in almost all the works dealing with piecewise smooth systems. In fact, since then the bifurcations occurring in a continuous piecewise linear system have been considered in many works, especially related to the map considered in these works, which is called two-dimensional border collision normal form map. We refer to [13–16] for the transition to chaotic dynamics, and to [17,18] for the bifurcations involving cycles with complex eigenvalues (a focus and a center). Other kinds of bifurcations peculiar of piecewise linear maps are those related to cycles with an eigenvalue -1 (also called degenerate flip bifurcation) or associated with periodic points which disappear reaching the boundary of the plane, infinity, and then becoming virtual, this is related to an eigenvalue $+1$ (also called degenerate transcritical bifurcation), as described in [19]. Moreover, a fold bifurcation in smooth maps is well known, it leads to a pair of cycles. Similarly occurs in continuous piecewise linear maps, a fold bifurcation may occur, leading to a pair of cycles, but in this case it is always related also to a border collision bifurcation, that is, at the bifurcation value one periodic point belongs to the set in which the map changes definition, so that the term fold border collision bifurcation is often used (for more details see [19]).

One more property, related to the different dynamic behaviors, refers to the invertibility or non-invertibility of the map in the phase plane. Recall that in invertible maps homoclinic orbits can be related only to saddle cycles (intersection between the stable and unstable sets), and the basins of attracting sets are always simply connected. Differently, in non-invertible maps the homo-

* Corresponding author. Tel.: +66851684930.
E-mail address: wirottik@psru.ac.th (W. Tikjha).

https://doi.org/10.1016/j.chaos.2020.109813

clinic orbits can occur also for repelling nodes or foci (related to snap-back repellers) and the basins of attraction can also be multiply connected or disconnected. The parameters at which a map changes between the invertible/non-invertible cases are particular, here called degenerate, because in such cases there exists a whole area which is mapped into a curve of the plane, the points of which have thus infinitely many rank-1 preimages. The dynamics occurring in similar degenerate cases are rarely considered in published papers. We refer to [20] for a relevant example.

The study of such degenerate cases in a continuous piecewise smooth two-dimensional map is the goal of the present paper. We consider a particular continuous system, already introduced in [21], the two-dimensional piecewise linear map given by

$$T: \begin{cases} x' = |x| - ay \\ y' = x - cy + d \end{cases} \tag{1}$$

where a, c, and $d > 0$ are real parameters, which is a particular case of a family of maps proposed in [22]. As it is shown in [21] the value of the parameter d is just a scaling factor, and we can consider $d = 1$ in the system given above. Moreover, in the same work the fixed points (real and virtual) have been determined together with the existence regions of pairs of 3-cycles and 4-cycles, and the regions related to invertible/non-invertible maps of the family. The parameters are varied in the (a, c) parameter plane. The degenerate cases occur for $c = a$ and $c = -a$, and at such values a whole half-plane is mapped into the critical line of map T (also called $Z_0 - Z_1 - Z_\infty$ case). This degeneracy, or peculiarity, allows us to determine parameter ranges at which a fixed point is globally attracting or a 3-cycle is almost globally attracting (i.e. attracting all the points of the phase plane except for a fixed point and a saddle 3-cycle whose stable set has a very simple structure).

After this Introduction, the structure of the paper is as follows. In Sec. 2 we describe some properties of map T related to the fixed points and 3-cycles, which are involved in the dynamics occurring in the degenerate cases here considered. The degenerate cases are considered in Sec. 3. First the simplest case, for $c = -a$, when the left partition $x < 0$ is mapped into the critical line LC, and we show that the real fixed point is globally attracting. In subsection 3.2 we consider the degenerate case $c = a$. The possible outcome of the dynamics are now very different. We have intervals of values (on $c = a$) in which the fixed point may be globally attracting, or coexisting with an attracting 3-cycle, and the related basins may be separated by a frontier with simple or complex (fractal) structure. But the main interval on $c = a$ leads to an almost globally attracting 3-cycle, which means attracting all the points of the phase plane except for a fixed point and a saddle 3-cycle whose stable set has a very simple structure. This can be proved by using the first retun map on the critical curve LC in the right partition. Moreover, by using a suitable first return map we show the appearance by fold border collision bifurcation of a pair of 5-cycles, one of which may be attracting and coexisting with the attracting 3-cycle. The related basins in the phase plane (x, y) are separated by sets with a complex structure. Sec. 4 concludes.

2. Preliminaries

We consider the two-dimensional piecewise linear map given by $(x', y') = T(x, y)$ defined in (1) with $d = 1$, as a function of the two parameters (a, c). This piecewise linear continuous map has a critical line in $x = 0$, denoted LC_{-1} (following [23]), separating the regions where the map has different definitions. Let us rewrite the system defined in the two partitions $x > 0$ and $x < 0$ (which are also called left/right partitions) as follows:

$$T := \begin{cases} T_L(x, y) & \text{if } x \le 0 \\ T_R(x, y) & \text{if } x > 0 \end{cases} \quad \text{where} \tag{2}$$

$$T_L(x, y) := \begin{cases} x' = -x - ay \\ y' = x - cy + 1 \end{cases}, \quad T_R(x, y) := \begin{cases} x' = x - ay \\ y' = x - cy + 1 \end{cases}. \tag{3}$$

Due to continuity, both functions T_L and T_R map the critical line LC_{-1} $(x = 0)$ onto the line given by

$$LC: \quad y = \frac{c}{a}x + 1, \text{for } a \neq 0. \tag{4}$$

As usual in piecewise smooth systems, the symbols R and L are used to denote the itinerary of a point (for the regions $x > 0$ and $x < 0$, respectively) and, in particular, the symbolic sequence of cycles. For a point belonging to the critical line LC_{-1} both symbols can be used; however, this case denotes a transition or bifurcation, and it is considered separately. For example, in the case of a cycle, the merging of a periodic point with LC_{-1} represents a collision, which may lead to a bifurcation (appearance/disappearance of the cycle).

It is well known that the dynamic behaviors highly depend on the invertibility/non-invertibility of the map[1] and, as evidenced in [21], considering the preimages of a point belonging to the right/left side of the LC curve and looking for their position with respect to the boundary $x = 0$, it is easy to prove the following:

Property 1. *Let $a > 0$.*

For $c > 0$ map T is invertible for $a > c$, otherwise it is non-invertible of $Z_0 - Z_2$ type;

for $c = a$ map T is degenerate, the half-plane $x > 0$ is mapped into the critical line LC $(y = x + 1)$, thus it is non-invertible of $Z_0 - Z_1 - Z_\infty$ type;

for $c < 0$ map T is invertible for $a > |c|$, otherwise it is non-invertible of $Z_0 - Z_2$ type;

for $c = -a$ map T is degenerate, the half-plane $x < 0$ is mapped into the critical line LC $(y = -x + 1)$, thus it is non-invertible of $Z_0 - Z_1 - Z_\infty$ type.

We consider the region $a > 0$ in order to have bounded dynamics for map T. So at the degenerate cases occurring for $c = a$ and $c = -a$, a whole half-plane is mapped onto the critical line, and the map is called of $Z_0 - Z_1 - Z_\infty$ type because each point of LC has infinitely many preimages (all the points of a half-line).

For $a > 0$ map T has a unique real fixed point

$$P_L^* = (x_L^*, y_L^*) = \left(-\frac{a}{2 + a + 2c}, \frac{2}{2 + a + 2c}\right) \tag{5}$$

while $P_R^* = (x_R^*, y_R^*) = (-1, 0)$ is always a virtual one. The stability analysis of P_L^* depends on the eigenvalues of the Jacobian matrix of the linear map T_L. We have

$$tr(J_L) = -(1 + c), \; D_L = det(J_L) = (a + c) \tag{6}$$

so that the characteristic polynomial $\mathcal{P}_L(\lambda)$ leads to $\mathcal{P}_L(-1) = a$, $\mathcal{P}_L(1) = 2 + a + 2c$ and the region in the (a, c) parameter plane in which P_L^* is an attracting fixed point, given by $\mathcal{P}_L(1) > 0$, $\mathcal{P}_L(-1) > 0$ and $D_L < 1$, corresponds to

$$S_L^* := \left\{a > 0, \; c > -\frac{a}{2} - 1 \;\; c < -a + 1\right\}. \tag{7}$$

In explicit form the eigenvalues are as follows:

$$\lambda_{1,2}(P_L^*) = \frac{1}{2}\left(-(1 + c) \pm \sqrt{(1 - c)^2 - 4a}\right). \tag{8}$$

The existence region of the real fixed point P_L^* is shown colored in the (a, c) parameter plane in Fig. 1(a), and the bright yellow

[1] In invertible maps homoclinic orbits can be related only to saddle cycles (intersection between the stable and unstable sets), and the basins of attracting sets are always simply connected. Differently, in non-invertible maps the homoclinic orbits can occur also for repelling nodes or foci (related to snap-back repellers) and the basins of attraction can also be multiply connected or disconnected.

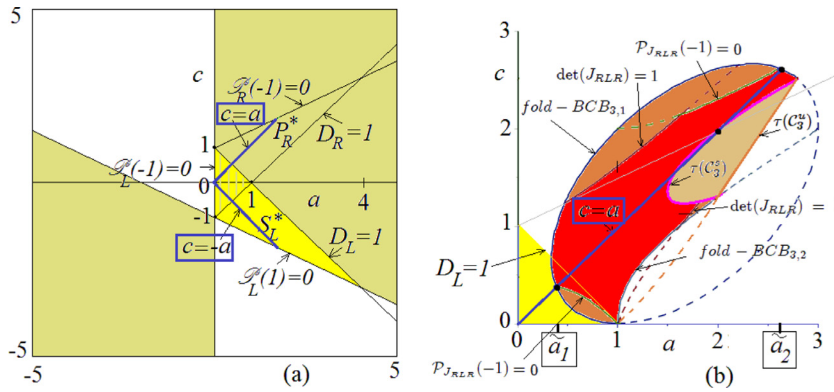

Fig. 1. In (a) the existence and stability regions of the fixed points are evidenced in the (a, c) parameter plane. In (b) the existence and stability regions of the 3-cycles are evidenced. The lines of equation $c = a$ and $c = -a$ which are of interest in this work are evidenced in blue.

triangle is the region S_L^* in which P_L^* is attracting. In the same figure we have also reported the boundaries of the existence region of the virtual fixed point, P_R^*, to evidence the character of the existing virtual fixed point P_R^* (attracting or repelling): since $tr(J_R) = (1 - c)$ and $D_R = det(J_R) = (a - c)$ the characteristic polynomial $\mathcal{P}_R(\lambda)$ leads to $\mathcal{P}_R(1) = a,\ \mathcal{P}_R(-1) = 2 + a - 2c$ and the region in the (a, c) parameter plane in which P_R^* is a virtual attracting fixed point is given by $\mathcal{P}_R(1) > 0,\ \mathcal{P}_R(-1) > 0$ and $D_R < 1$, that is $S_R^* := \left\{a > 0,\ c < \frac{a}{2} + 1\ \ c > a - 1\right\}$. In particular, the virtual fixed point P_R^* is attracting for $0 < a < 1$ and $c < (1 - a)$.

The existence of an attracting virtual fixed point P_R^*, or a repelling focus, implies that the trajectories from the right partition are always mapped in the left partition in a finite number of iterations. This creates the possibility to have attracting cycles with periodic points in both partitions, coexisting with the attracting fixed point P_L^*. And in fact, in our system, we have an existence region of a pair of 3-cycles, which overlaps with that of the fixed point P_L^*, and in part with the stability region of P_L^*. This has been shown in [21]. We determine the existence of a 3-cycle of map T looking for the solutions of the equation $T^3(x, y) = (x, y)$ noting that the symbolic sequence of the two cycles are RLR and RLL, and when they are merging we have RLC denoting with C a point on the critical line LC_{-1}. Considering particular solutions of the equation $T^3(x, y) = (x, y)$, two 3-cycles with symbolic sequence RLR and RLL can be determined. A periodic point of a real 3-cycle $\mathcal{C}_3^s$ which may be attracting is given by

$$(x_{3,1}^s, y_{3,1}^s) = \left(\frac{a(-c^2 - a^2 + ac + 2a + c - 1)}{2c^3 + a^3 - a^2c - c^2a - 3ac + a + 2},\right.$$
$$\left.\frac{2(c^2 - c - ac + a + 1)}{2c^3 + a^3 - a^2c - c^2a - 3ac + a + 2}\right) \tag{9}$$

and satisfies $T_R \circ T_L \circ T_R(x, y) = (x, y)$ where

$$T_R \circ T_L \circ T_R(x, y) = \begin{bmatrix} (ac - 2a - 1) & (ac + a - ac^2 + a^2) \\ (-a - c + c^2 + 1) & (a + 2ac - c^3) \end{bmatrix} \begin{bmatrix} x \\ y \end{bmatrix}$$
$$+ \begin{bmatrix} -2a + ac \\ -a - c + c^2 + 1 \end{bmatrix}. \tag{10}$$

Considering

$$T_L \circ T_R \circ T_L(x, y) = \begin{bmatrix} 2a + 1 + ac & -c^2a - ac + a^2 + a \\ c - a + c^2 - 1 & 2ac - a - c^3 \end{bmatrix} \begin{bmatrix} x \\ y \end{bmatrix}$$
$$+ \begin{bmatrix} ac \\ c^2 - a - c + 1 \end{bmatrix} \tag{11}$$

and solving for $T_L \circ T_R \circ T_L(x, y) = (x, y)$ a periodic point $(x_{3,1}^u, y_{3,1}^u)$ of a real 3-cycle $\mathcal{C}_3^u$ (which is repelling) is obtained, given by

$$(x_{3,1}^u, y_{3,1}^u) = \left(\frac{-(a^2 - ac + c - c^2 - 1)}{a^2 + ac - 3c - c^2 - 1}, \frac{2(a - 1)}{a^2 + ac - 3c - c^2 - 1}\right). \tag{12}$$

The two 3-cycles appear/disappear via fold border collision bifurcation at a parameter point (a, c) for which it is $x_{3,1}^s = 0$, and for $a \neq 0$ this leads to the necessary condition

$$fold - BCB_{3,1} : c^2 + a^2 - ac - 2a - c + 1 = 0 \tag{13}$$

and another fold border collision bifurcation occurs considering the numerator of $x_{3,1}^u$ in (12), for

$$fold - BCB_{3,2} : a^2 - ac + c - c^2 - 1 = 0. \tag{14}$$

The existence region of the pair of 3-cycles is also bounded by a curve related to a degenerate transcritical bifurcation occurring when one eigenvalue becomes 1 and the periodic points of the cycles tend to infinity. For the 3-cycle $\mathcal{C}_3^s$ this occurs when the parameter point (a, c) belongs to the curve denoted by $\tau(\mathcal{C}_3^s)$:

$$\tau(\mathcal{C}_3^s)\ :\ 2c^3 + a^3 - a^2c - c^2a - 3ac + a + 2 = 0 \tag{15}$$

while for the other 3-cycle saddle $\mathcal{C}_3^u$ the degenerate transcritical bifurcation occurs for:

$$\tau(\mathcal{C}_3^u)\ :\ a^2 + ac - 3c - c^2 - 1 = 0. \tag{16}$$

These curves are shown in Fig. 1(b). Inside the existence region, the stability region of $\mathcal{C}_3^s$ is bounded by bifurcation curves related to the center bifurcations and degenerate flip bifurcations, so that these can be determined from the eigenvalues of the function $T_R \circ T_L \circ T_R(x,\ y)$, for which we have $tr(J_{RLR}) = 3ac - c^3 - a - 1$ and $\det(J_{RLR}) = (a - c)^2(a + c)$. The stability conditons are $\mathcal{P}_{J_{RLR}}(1) = 2c^3 + a^3 - a^2c - c^2a - 3ac + a + 2 > 0,\ \mathcal{P}_{J_{RLR}}(-1) = a(a^2 - c^2 - ac + 3c - 1) > 0$ and $\det(J_{RLR}) < 1$ leading to the red portion shown in Fig. 1(b).

In particular, as evidenced in Fig. 1(b), the degenerate line $a = c$ which is of interest in this work, crosses the existence region of both the fixed point P_L^* and the 3-cycles, and involves three particular codimension-two bifurcation points (black points in Fig. 1(b)), which shall characterize the dynamics, as described in the next section.

3. Degenerate cases of non-invertibility

The system we consider is characterized by several regions in the parameter space (a, c) of coexisting cycles, and it is interesting to show that also in the degenerate cases the dynamics may be not trivial. Due to the degeneracy, for $c = a,\ a > 0$, then any trajectory crossing the right partition, or for $c = -a,\ a > 0$, any trajectory crossing the left partition, is mapped onto a single straight line: the critical line LC. In such cases, we have that any trajectory crossing the partition ($x > 0$ or $x < 0$) must have the $\omega-$limit set belonging to the images of the critical line. This may allow for the use of same one-dimensional map representing the first return on the critical line LC or some portions of it.

3.1. Case $c = -a$

Let us first consider the parameters belonging to $c = -a$ in the range $0 < a < 2$ (that is, inside the stability region of P_L^*) at which the left partition $x < 0$ is mapped into the critical line LC, which has a negative slope ($y = -x + 1$) and the real fixed point $P_L^* = (x_L^*, y_L^*) = (-\frac{a}{2-a}, \frac{2}{2-a}) \in LC$ is attracting. Its eigenvalues are $\lambda_1(P_L^*) = 0$ and $\lambda_2(P_L^*) = a - 1$ which is negative for $a < 1$ and positive for $1 < a < 2$ (with eigenvector along LC). The virtual fixed point P_R^* is attracting for $0 < a < \frac{1}{2}$, a repelling focus for $\frac{1}{2} < a < 2$. Any initial condition on the right side has the trajectory which is mapped in a finite number of iterations to the left side, so we can consider the points of the left partition which are mapped onto the straight line LC.

For a point $(z, -z+1) \in LC$ with $z < 0$, we have $T_L(z, -z+1) = (z(a-1) - a, -z(a-1) + a + 1)$ which belongs to LC in the left partition for $a \geq 1$ or $a < 1$ and $-\frac{a}{1-a} < z < 0$. For $a \geq 1$ it is $\lambda_2 \geq 0$, so the trajectory necessarily converges monotonously to P_L^*. Differently, for $0 < a < 1$ the eigenvalue satisfies $-1 < \lambda_2 < 0$ and since $T_L(-\frac{a}{1-a}, \frac{a}{1-a} + 1) = (0, 1)$ all the trajectories of the interval $-\frac{a}{1-a} \leq z < 0$ are converging to P_L^* without crossing the right partition. For $z < -\frac{a}{1-a}$ the trajectory crosses the right partition, in which the action of the virtual fixed point applies, which is a contraction for $0 < a < \frac{1}{2}$, or P_R^* is repelling focus for $\frac{1}{2} < a < 2$ and it can be shown that in at most 5 iterations the trajectory either stays in the left partition or it is mapped again in the right partition of LC but closer to $x = 0$ so that in a few iterations the trajectory enters the interval $-\frac{a}{1-a} \leq z < 0$. We have so proved the following

Proposition 1. *Let $c = -a$ and $0 < a < 2$, then the fixed point P_L^* is globally attracting.*

It is worth noting that the extrema of the interval (i.e. $a = 0$ and $a = 2$) are excluded from the above proposition because these are bifurcation values, and are considered separately. From the first coordinate of P_L^* we can see that it crosses the border $x = 0$ when the parameter a changes sign, from negative to positive or *vice versa*. Moreover, from the expression of the eigenvalues given in (8) we also have that for $a = 0$ the eigenvalues become $\lambda_1 = -1$ and $\lambda_2 = -c$. Thus, crossing the boundary $a = 0$ of the stability region from inside we have that the fixed point becomes virtual exactly when one eigenvalue crosses -1. After that, for a parameter point (a, c) belonging to the white region of Fig. 1(a), we have both fixed points which are virtual and repelling, and map T has divergent orbits.

Differently, the value $a = 2$ corresponds to the crossing of the lower boundary $\mathcal{P}_L(1) = 2 + a + 2c = 0$ from inside, as shown in Fig. 1(a), so that one eigenvalue approaches 1 and also the denominator of the expression of the fixed point in both components tends to zero, that is, the fixed point tends to infinity. Thus, it corresponds to a degenerate transcritical bifurcation [19], after which the fixed point disappears (i.e. it becomes virtual), and the generic trajectory of map T is divergent.

3.2. Case $c = a$

A different behavior occurs in the other transition, for $c = a$. The right partition $x > 0$ is mapped onto the critical line LC, which is now a straight line with a positive slope ($y = x + 1$), and the real fixed point P_L^* (attracting or repelling) does not belong to LC, and it is always located below LC. Now a point of LC is represented as $(z, z+1)$.

The virtual fixed point P_R^* is attracting for $0 < a < 2$, and its eigenvalues are $\lambda_1(P_R^*) = 0$ and $\lambda_2(P_R^*) = 1 - a$ which is positive for $a < 1$ and negative otherwise.

The fixed point P_L^* is attracting for $0 < a < 0.5$, and a repelling focus for $a > 0.5$ in the range here considered (the eigenvalues are complex for $3 - 2\sqrt{2} < a < 3 + 2\sqrt{2}$).

Since for $0 < a < 0.5$ the functions in the two partitions are both contractions, we may expect global convergence to the real fixed point P_L^*. Any point in the right partition is mapped on LC and since $\lambda_2(P_R^*)$ is positive the iterates stay on LC on the right side up to a point with $0 \leq z \leq \frac{a}{1-a}$ from which it is mapped on the left side in a point with $-a \leq z \leq 0$. From the left side either it converges to P_L^* without crossing the right partition or it may be mapped again in the right side. Since we know that a pair of 3-cycles exists in this range of parameter values (appearing via fold-BCB when the conditions in eq. (13) are satisfied, that is for $a = \widetilde{a}_1 \simeq 0.381966$), we look for a suitable first return map on LC revealing their appearance and existence.

Considering a point $(z, 1+z) \in LC$ with $z > 0$ we have $T_R(z, z+1) = (z(1-a) - a, z(1-a) - a + 1) \in LC$ which belongs to the region $x < 0$ if $a \geq 1$ while for $a < 1$ this holds if $0 < z < \frac{a}{1-a}$. Then we have $T_L \circ T_R(z, z+1) = (z(a^2 - 1) + a^2, (1-a)^2(z+1))$ which belongs to the region $x > 0$ if $a \geq 1$ while for $a < 1$ this holds if $0 < z < \frac{a^2}{1-a^2}$. Then we consider $T_R \circ T_L \circ T_R(z, z+1) = (z', z'+1)$ given by $z' = m_r z + q$ where $m_r = -a^3 + 3a^2 - a - 1$ and $q = m_r + 1 = -a^3 + 3a^2 - a$. If $z' > 0$ then this is the first return on LC, under the given conditions. As we shall see below, the restrictions considered so far are satisfied in our region of interest for $\widetilde{a}_1 < a \leq 1 + \sqrt{2}$, while the case $a > 1 + \sqrt{2}$ requires further analysis, as described below.

For the left partition, considering $z < 0$ we determine the first return map of T on LC. It is $T_L(z, z+1) = (-z(1+a) - a, z(1-a) + 1 - a)$ which belongs to the left partition for $-\frac{a}{1+a} < z < 0$, then $T_L \circ T_L(z, z+1) = (z(1+a^2) + a^2, z(a^2 - 2a - 1) + a^2 - 2a + 1)$ which belongs to the right partition for $-\frac{a^2}{1+a^2} < z < 0$, then $T_R \circ T_L \circ T_L(z, z+1) = (z', z'+1) \in LC$ where $z' = m_l z + q$ with $m_l = -a^3 + 3a^2 + a + 1$ and $q = -a^3 + 3a^2 - a$. We can so consider the first return map on LC via the one-dimensional map $z' = f(z)$ defined as follows:

$$f(z) : \begin{cases} z' = m_l z + q \text{ if } z \leq 0 \\ z' = m_r z + q \text{ if } z \geq 0 \end{cases} \tag{17}$$

where

$$\begin{aligned} m_l &= -a^3 + 3a^2 + a + 1, \\ m_r &= (a-1)(1 + 2a - a^2), \\ q &= m_r + 1 = a(-a^2 + 3a - 1). \end{aligned} \tag{18}$$

The analysis of this one-dimensional piecewise linear map leads to the following results: the slope m_r belongs to the interval $[-1, 1]$ iff $q \in [0, 2]$ and this occurs iff $\widetilde{a}_1 \leq a \leq \widetilde{a}_2$ with $\widetilde{a}_1 \simeq 0.381966$, $\widetilde{a}_2 \simeq 2.618$ ($\widetilde{a}_1$ and $\widetilde{a}_2$ are the two roots of $(-a^2 + 3a - 1) = 0$), while it is $m_l > 1$ for any a satisfying $\widetilde{a}_1 \leq a \leq \widetilde{a}_2$. We remark that on the line $c = a$, shown in Fig. 1(b), the point $a = \widetilde{a}_1$ corresponds to the codimension-2 parameter point in which the BCB bifurcation curve and the degenerate flip bifurcation curve related to the 3-cycles are intersecting, the point $a = 2$ corresponds to the unique point on the line $c = a$ in which the attracting 3-cycle undergoes a transcritical bifurcation becoming infinite (and also the virtual fixed point P_R^* changes from attracting to repelling with one real eigenvalue smaller that -1), while the point $a = \widetilde{a}_2$ corresponds to the second codimension-2 parameter point in which the BCB bifurcation curve and the degenerate flip bifurcation curve related

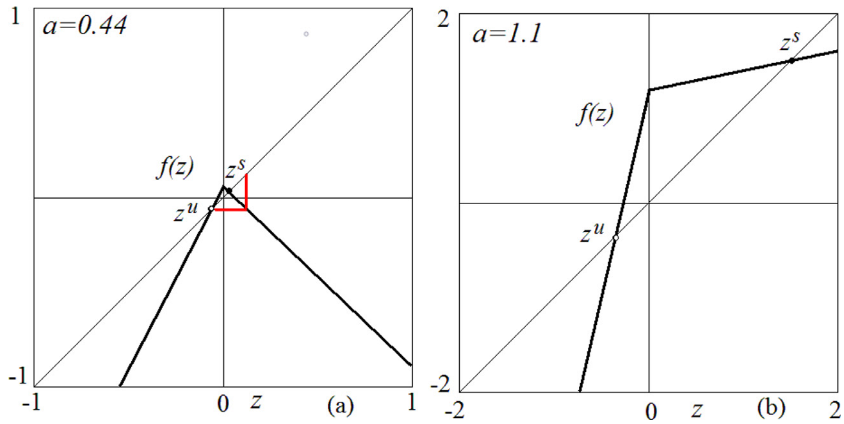

Fig. 2. Shape of the one-dimensional map $f(z)$ in the degenerate case $a = c$. In (a) the attracting 3-cycle $\mathcal{C}_3^s$, represented by the fixed point, coexists with the attracting fixed point P_L^*. In (b) the 3-cycle $\mathcal{C}_3^s$ is almost globally attracting.

to the 3-cycles are intersecting. Moreover, m_r takes its maximum value ($m_r = 1$) at $a = 2$, and it is:

$$\begin{array}{ll} m_r = -1 \text{ for } a = \widetilde{a}_1 & -1 < m_r < 0 \text{ for } \widetilde{a}_1 < a < 1 \\ m_r = 0 \quad \text{for } a = 1 & 0 < m_r < 1 \text{ for } 1 < a < 2 \\ m_r = 1 \quad \text{for } a = 2 & 1 > m_r > 0 \text{ for } 2 < a < 1 + \sqrt{2} \\ m_r = 0 \quad \text{for } a = 1 + \sqrt{2} & 0 > m_r > -1 \text{ for } 1 + \sqrt{2} < a < \widetilde{a}_2 \\ m_r = -1 \text{ for } a = \widetilde{a}_2. & \end{array} \tag{19}$$

For $0 < a < \widetilde{a}_1$ the fixed point P_L^* is globally attracting (the first return map in the right side is not applicable, all the points ultimately remain in the left partition). The fold-BCB occurring at $a = \widetilde{a}_1$ is related to a codimension-2 point because the slope on the right partition is $m_r = -1$, leading for $a > \widetilde{a}_1$ to a pair of fixed points, one $z^s > 0$ attracting with negative slope, as shown in the graph of the map $z' = f(z)$ in Fig. 2(a), and the basin of attraction of z^s is bounded by the repelling fixed point on the left side, z^u, and its rank-1 preimage. Clearly the positive fixed point corresponds to the periodic point of the attracting 3-cycle $\mathcal{C}_3^s$, since it is $z^s = x_{3,1}^s$, while the negative fixed point is $z^u = x_{3,1}^u$, the point of the repelling 3-cycle $\mathcal{C}_3^u$ of map T.

In the one-dimensional map $f(z)$ a point mapped in $z < z^u$ has a divergent trajectory, but in the two-dimensional map T such points have a different behavior. In fact, the map $z' = f(z)$ represents the first return on LC only for the trajectories of T which follow the symbolic sequence RLR starting from the right side and LLR starting from the left side of the critical point $(0, 1) \in LC$ (corresponding to $z = 0$). For $\widetilde{a}_1 < a < 1$ this is clearly true in a neighborhood of $z = 0$, but not everywhere, since we know that as long as P_L^* is attracting (for $0 < a < 0.5$) there are regions of points having the trajectory completely on the left partition, and points in the right side exist which are mapped in these regions. The value $a = 0.5$ corresponds to the center bifurcation of P_L^*, which has been shown in [21] is of supercritical type.

For $\widetilde{a}_1 < a < 0.5$ the first return map $z' = f(z)$ is clearly meaningful in the interval $(z^u, f^{-1}(z^u))$ and in the two-dimensional map this gives the immediate basin of z^s on LC. The stable set of the saddle 3-cycle $\mathcal{C}_3^u$ separates the points belonging to the basins $\mathcal{B}(\mathcal{C}_3^s)$ and $\mathcal{B}(P_L^*)$ while for $a = 0.5$ the stable set of the saddle 3-cycle $\mathcal{C}_3^u$ separates the points belonging to the basins $\mathcal{B}(\mathcal{C}_3^s)$ and the set of points which are mapped into closed invariant curves around the center P_L^*. Examples of these two cases are shown in Fig. 3: in Fig. 3(a) the fixed point is attracting (its basin is evidenced in yellow), while Fig. 3(b) shows the center bifurcation value. The outermost invariant closed curve around P_L^* is the envelope of all the images of the critical segments, and the white points denote those which are mapped in the invariant region around the center P_L^*.

For $a > 0.5$ after the supercritical center bifurcation, coexisting with the attracting 3-cycle an attracting closed curve Γ_+ exists, which is made of critical segments (when the rotation number is rational, so that the critical segments of the invariant curve are also a saddle-attracting node connection) or the invariant curve is the envelope of critical segments (when the rotation number is irrational). An example of the first kind is shown in Fig. 3(c), where the attracting set is a cycle of period 8. Clearly, increasing the parameter a several periodicity regions are crossed (which in the parameter plane (a, c) are issuing from the center bifurcation curve of P_L^*). The closed curve increases, approaching the boundary of its basin of attraction, which is given by the stable set of the saddle 3-

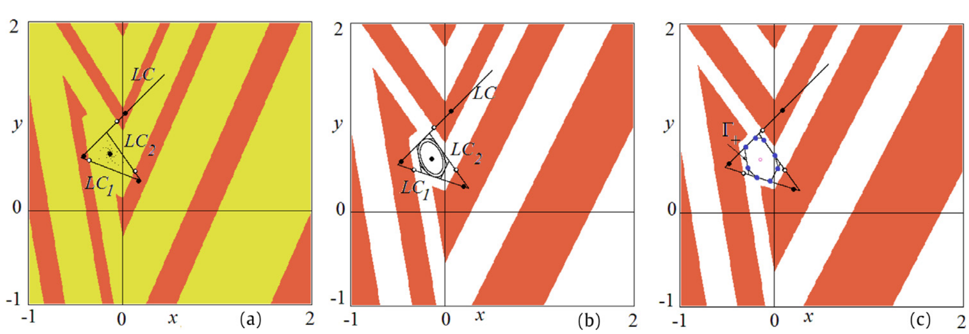

Fig. 3. Phase space at parameters close to the center bifurcation in the degenerate case $a = c$. In (a) $a = 0.44$, the attracting 3-cycle $\mathcal{C}_3^s$ coexists with the attracting fixed point P_L^*. In yellow the basin of the fixed point, in red the basin of $\mathcal{C}_3^s$ separated by the stable set of the saddle $\mathcal{C}_3^u$. In (b) $a = 0.5$ is the bifurcation value, an invariant area is filled with ellipses, the external one is the envelope of critical segments. In (c) $a = 0.52$ an attracting closed curve Γ_+, connection of a saddle and attracting node of period 8, also made up of critical segments, coexists with the 3-cycle $\mathcal{C}_3^s$, the basins are separated by the stable set of the saddle $\mathcal{C}_3^u$.

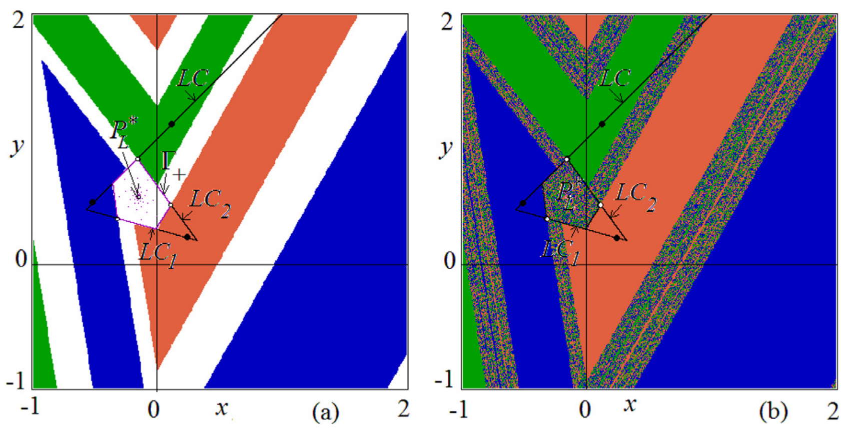

Fig. 4. In (a) $c = a = 0.564$ an attracting closed curve made up of critical segments is very close to the basin boundary. One branch of the 3-cycle saddle $\mathcal{C}_3^u$ is close to an homoclinic bifurcation. The basin of the attraction of the 3-cycle $\mathcal{C}_3^s$ is shown with three colors, for map T^3 in white the basin of the closed curve. In (b) $c = a = 0.565$ after the contact the closed curve no longer exists, the basins of the fixed points of $\mathcal{C}_3^s$ for map T^3, shown with three colors, are separated by the stable set of the saddle $\mathcal{C}_3^u$, and has now a fractal structure.

cycle $\mathcal{C}_3^u$. In Fig. 4(a) we show the closed curve very close to such a contact bifurcation, the critical segments belonging to the attracting closed curve are almost on segments belonging to the stable set of the 3-cycle saddle. The basin of the 3-cycle is considered for the map T^3, so to better evidence the basins of the three fixed points of map T^3, while the white points are still converging to the closed curve Γ_+.

The contact bifurcation is clearly a homoclinic bifurcation of the saddle 3-cycle: after the contact the stable and unstable sets are intersecting transversely, leading to the existence of a chaotic set (a chaotic repeller) since the homoclinic points prove the existence of infinitely many repelling cycles. This is shown in Fig. 4(b): soon after the contact, the fractal structure of the basins of the three fixed points of map T^3 fills the former basin of the closed curve.

As the parameter a approaches 1, the complex structure of the basins simplifies. In fact, as we have seen above, for $a \geq 1$ as long as the slope m_r is positive, or non-negative (i.e. for $1 \leq a \leq 1 + \sqrt{2}$) any point belonging to the right side of LC, say LC_+, is mapped again to this side in three iterations. For any $z > 0$ $T_R \circ T_L \circ T_R(z, z+1) = (z', z'+1) \in LC_+$ and this implies that map $f(z)$ is the proper first return on LC_+, Fig. 2(b) shows the function when the fixed point on the right side is related to a positive slope, and it attracts all the points on the right side of the unstable fixed point z^u. It follows that the 3-cycle $\mathcal{C}_3^s$ is the only attracting set, almost globally attracting as described in the following

Proposition 2. *Let $c = a$ and $1 \leq a \leq 1 + \sqrt{2}$ then the 3-cycle $\mathcal{C}_3^s$ attracts all the points of the phase plane except for the saddle 3-cycle C_3^u and its stable set, which has a simple structure issuing from P_L^*.*

Proof. The structure of the basins of the three points of C_3^s, as fixed points of T^3, is determined by the stable sets of the three fixed points of the saddle C_3^u, which is given by the local stable set and its preimages. In the considered case also the points of the 3-cycles have one eigenvalue equal to zero (since it is $D_R = 0$), which corresponds to the stable set, given by the related eigenvector. Clearly, the other eigenvalue is related to the stability/instability of the point, and the related eigenvector is on the critical line crossing the point. Let us consider the point $(x_{3,1}^u, y_{3,1}^u)$ of the 3-cycle saddle as given in (12), fixed point of $T_L \circ T_R \circ T_L(x, y)$ given in (11). From that function, for $c = a$, we obtain the following system

$$T_L \circ T_R \circ T_L(x, y) = \begin{bmatrix} (a+1)^2 & a(1-a^2) \\ -(1-a^2) & -a(a-1)^2 \end{bmatrix} \begin{bmatrix} x \\ y \end{bmatrix} + \begin{bmatrix} a^2 \\ a^2 - 2a + 1 \end{bmatrix} \tag{20}$$

whose fixed point is $(x_{3,1}^u, y_{3,1}^u)$ and the related eigenvalues are $\lambda_1(x_{3,1}^u, y_{3,1}^u) = 0$ and $\lambda_2(x_{3,1}^u, y_{3,1}^u) = (a+1)^2 - a(a-1)^2 > 1$ for any value of a in the considered interval. The local eigenvector related to the zero eigenvalue is a straight line issuing from the point $(x_{3,1}^u, y_{3,1}^u)$ with slope

$$s(x_{3,1}^u, y_{3,1}^u) = \frac{a+1}{a(a-1)} \tag{21}$$

It can be seen that for $a < 1$ it is $s(x_{3,1}^u, y_{3,1}^u) < 0$ so that the locally stable set intersects the critical line LC_{-1}, and this implies that the global stable set (taking all the preimages) may become a set with complex structure (as shown in the examples of Fig. 3). For $a = 1$ the slope becomes infinite, which means that the local stable set becomes the vertical straight line issuing from $(x_{3,1}^u, y_{3,1}^u) = (-\frac{1}{3}, 0)$ which does not intersect LC_{-1}. It crosses the axis $y = 0$ for $x = -\frac{1}{3} < 0$ and the preimages are only in the left side, converging to P_L^*, so that the global stable set does not intersect any critical line. The same holds for the stable sets of the other point in the left partition. For the point in the right partition the slope of the stable set is given by $m = \frac{1}{a}$ and it intersects the critical line LC_{-1} in a point of the segment [0,1), but since it belongs to the right partition, all the points of this line for $x \geq 0$ are mapped into the point of C_3^u on the left side. Thus the three basins of attraction are three simply connected regions covering the whole plane. Similar simple structure exists for $a > 1$, it can be described as long as the stable set issuing from $(x_{3,1}^u, y_{3,1}^u)$ is not intersecting LC, that is, when the slope is positive and greater than 1 (an example is shown in Fig. 5(a)). From, the slope given in (21) it follows that $s(x_{3,1}^u, y_{3,1}^u) = 1$ for $a = 1 + \sqrt{2}$. Thus for $1 \leq a \leq 1 + \sqrt{2}$ the basin of attraction has the simple structure as described above, while for $a > 1 + \sqrt{2}$ the stable set is intersecting again the critical curves and the structure of the basins increases in complexity (an example is shown in Fig. 5(b)). □

For $1 + \sqrt{2} < a < \widetilde{a}_2$ the slope m_r becomes negative again, and it is possible to have $T_R \circ T_L \circ T_R(z, z+1) = (z_1, z_1+1)$ with $z_1 = m_r z + q < 0$, which occurs for $z > \frac{q}{|m_r|}$. When this occurs it is possible to have different symbolic sequences for the first return map on LC, and to have the first return on the right side of LC we have to continue the applications of the map.

Considering $T_L \circ T_R \circ T_L \circ T_R(z, z+1) = (-z_1(1+a) - a, z_1(1-a) + 1 - a)$ with $z_1 = m_r z + q < 0$ we have a point belonging to the right partition for $|z_1| > \frac{a}{1+a}$ and we obtain the first return map with one more branch defined via $T_R \circ T_L \circ T_R \circ T_L \circ T_R(z, z+1) = (z', z'+1)$ with $z' = -(m_r z + q)(1 + 2a - a^2) - 2a + a^2$. We can so

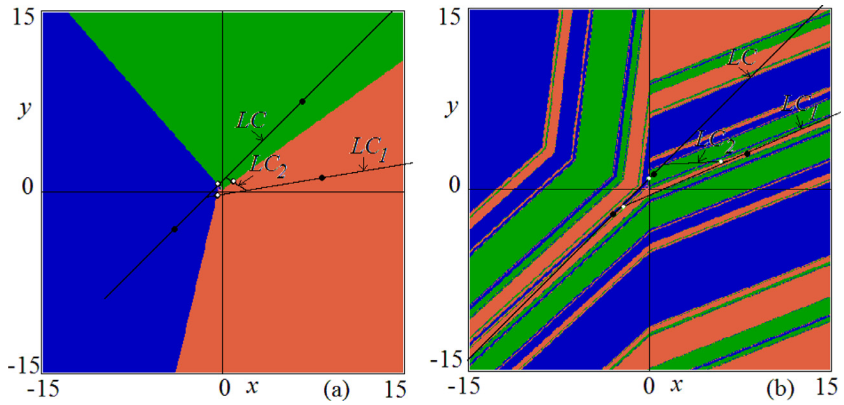

Fig. 5. In (a) $c = a = 1.4$ the 3-cycle $\mathcal{C}_3^s$ is almost globally attracting, the basins of the fixed points of $\mathcal{C}_3^s$ for map T^3, shown with three colors, are separated by the stable set of the saddle $\mathcal{C}_3^u$, which has a very simple structure. In (b) $c = a = 2.5351(> 1 + \sqrt{2})$ the 3-cycle $\mathcal{C}_3^s$ is attracting but the basins of the fixed points of $\mathcal{C}_3^s$ for map T^3 have now a more complex structure.

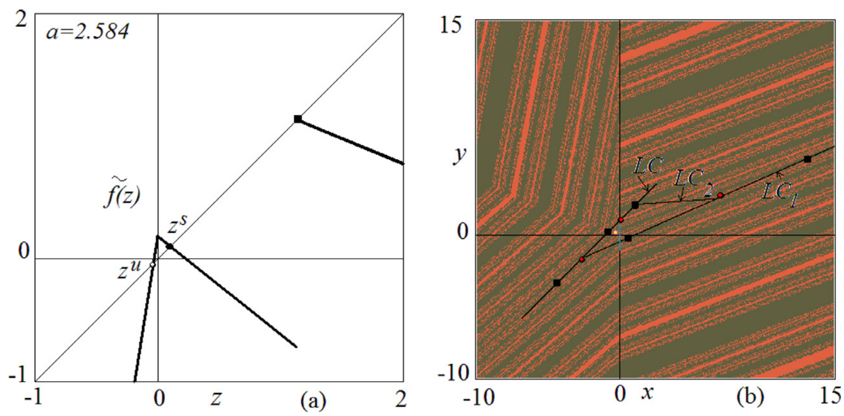

Fig. 6. In (a) shape of the one-dimensional map $\widetilde{f}(z)$ when the rightmost branch leads to the appearance of a new fixed point, at $a = 2.584$, attracting 5-cycle for map T. In (b) phase space of map T at $a = 2.6$ showing in red the basin of attraction of the 3-cycle $\mathcal{C}_3^s$, and in dark gray the basin of attraction of the coexisting attracting 5-cycle $\mathcal{C}_5^s$.

consider the map on LC via the one-dimensional map $z' = \widetilde{f}(z)$ defined as follows:

$$\widetilde{f}(z) : \begin{cases} z' = m_l z + q \text{ if } z \le 0 \\ z' = m_r z + q \text{ if } z \ge 0 \text{ and } m_r z + q > -\frac{a}{1+a} \\ z' = -(m_r z + q)(1 + 2a - a^2) - 2a + a^2 \text{ if } z > 0 \text{ and} \\ \qquad m_r z + q < -\frac{a}{1+a} \end{cases}$$

Considering the parameter a for values $a > 1 + \sqrt{2}$ the shape of the map $\widetilde{f}(z)$ is shown in Fig. 6(a). It does not represent the first return map in the interval of the right branch in which it becomes negative ($-\frac{a}{1+a} < m_r z + q < 0$) but it is the first return map for $m_r z + q < -\frac{a}{1+a}$ leading to the rightmost branch of the map, and from this branch it can be seen that for $a \simeq 2.584 < \widetilde{a}_2$ a pair of 5-cycles appears (via a new attracting fixed point of $\widetilde{f}(z)$, representing a fixed point of the function $T_R \circ T_L \circ T_R \circ T_L \circ T_R(x, y)$). The symbolic sequences (when starting from the points colliding with LC_{-1}) of the pair of cycles of map T is given by *RRLRL* and *LRLRL*, and the first one corresponds to an attracting 5-cycle $\mathcal{C}_5^s$, coexisting with $\mathcal{C}_3^s$. Obviously, all the periodic points of the cycles $\mathcal{C}_3^s$, $\mathcal{C}_3^u$, $\mathcal{C}_5^s$, $\mathcal{C}_5^u$ belong to critical segments of LC^i, $i \ge 1$ (which all belong to three segments of straight lines). An example for $a = 2.6 < \widetilde{a}_2$ is shown in Fig. 6(b), and the attracting 3-cycle is close to the fold-BCB, occurring at $a = \widetilde{a}_2$, leading to the disappearance of the pair of 3-cycles, and leaving the 5-cycle as unique attracting set.

4. Conclusions

In this work we have considered degenerate cases occurring in a family of piecewise smooth continuous two-dimensional maps at the transition from invertible to non-invertible, or *vice versa*. The degeneracy consists in an half plane which is mapped into a straight line. For the map defined in (2), the degenerate cases occur for $c = a$ and $c = -a$, and the whole half-plane $x > 0$ or $x < 0$, respectively, is mapped into the critical line LC of map T, also called $Z_0 - Z_1 - Z_\infty$ case since each point of LC has the rank-1 preimage which consists in a whole half-line. This degeneracy is peculiar because in some cases (and always when the fixed point is repelling) the $\omega-$ limit set of the trajectories must be on the images of the involved arc of LC, and thus the first return map on LC may be very useful to determine the dynamic behavior. This has been used in Sec. 3.1 to prove that for $c = -a$ in the region of interest (that is, when the dynamics are bounded), the real fixed point is globally attracting. In Sec. 3.2 we use the first return map on LC to prove that for $c = a$ in the main interval $1 \le a \le 1 + \sqrt{2}$ there exists a 3-cycle which attracts almost all the points of the phase plane, that is, all the points except for a fixed point and a saddle 3-cycle whose stable set has a very simple structure, consisting in three half-lines, and three simple curves issuing from the repelling fixed point. Moreover, the first return map allows us to predict the appearance by fold border collision bifurcation of a pair of 5-cycles, say at $a = a_5^*$, one of which may be attracting and coexisting with the attracting 3-cycle.

Our analysis is however not complete. In fact, there is an interval of values for a, $1 + \sqrt{2} < a < a_5^*$, at which the first return map described in Sec. 3.2 is not a complete characterization of the dynamics of map T, since it is not simple to detect the symbolic sequence of the trajectories, before their return on LC. These investigations are left for future works.

Declaration of Competing Interest

The authors declare that they have no known competing financial interests or personal relationships that could have appeared to influence the work reported in this paper.

CRediT authorship contribution statement

Laura Gardini: Conceptualization, Methodology, Software, Writing - original draft. **Wirot Tikjha:** Software, Validation, Writing - review & editing.

Acknowledgments

The work of first author has been done within the activities of the GNFM (National Group of Mathematical Physics, INDAM Italian Research Group). The second author is supported by the Centre of Excellence in Mathematics, National Research Council of Thailand, Thailand Science Research and Innovation and Pibulsongkram Rajabhat University, and is grateful to the University of Urbino for the hospitality during his visiting period.

References

[1] Banerjee S, Verghese G. Nonlinear Phenomena in Power Electronics, Attractors, Bifurcations, Chaos, and Nonlinear Control. 1. New York: Wiley-IEEE Press; 2001.
[2] Zhusubaliyev Z, Mosekilde E. Bifurcations and Chaos in piecewise-smooth dynamical systems, Nonlinear Science A,Vol. 44. 1. Singapore: World Scientific; 2003.
[3] Brogliato B. Nonsmooth mechanics models, dynamics and control. 1. New York: Springer-Verlag; 1999.
[4] di Bernardo M, Budd CJ, Champneys AR, Kowalczyk P. Piecewise-smooth Dynamical Systems: Theory and Applications, Applied Mathematical Sciences Vol. 163. 1. New York: Springer-Verlag; 2008.
[5] Ma Y, Agarwal M, Banerjee S. Border collision bifurcations in a soft impact system. Phys Lett A 2016;354:281–7.
[6] Radi D, Gardini L, Avrutin V. The role of constraints in a segregation model: The symmetric case. Chaos Solitons & Fractals 2014;66:103–11.
[7] Radi D, Gardini L. Entry limitations and heterogeneous tolerances in a schelling-like segregation model. Chaos Solitons & Fractals 2015;79:130–44. doi:10.1016/j.chaos.2015.07.009.
[8] Radi D, Gardini L. A piecewise smooth model of evolutionary game for residential mobility and segregation. CHAOS 2018;28:30–144. doi:10.1063/1.5023604.
[9] Burr C, Gardini L, Szidarovszky F. Discrete time dynamic oligopolies with adjustment constraints. Journal of Dynamics and Games 2015;2(1):65–81. doi:10.3934/jdg.2015.2.65.
[10] Gardini L, Sushko I, Matsuyama K. 2d discontinuous piecewise linear map: Emergence of fashion cycles fashion model. CHAOS 2018;28. doi:10.1063/1.5018588.
[11] Nusse H, JAYorke. Border-collision bifurcations including 'period two to period three' bifurcation for piecewise smooth systems. Physica D 1992;57:39–57.
[12] Nusse H, JAYorke. Border-collision bifurcations for piecewise smooth one dimensional maps. Int J Bifurcation Chaos 1995;5:189–207.
[13] Banerjee S, Yorke JA, Grebogi C. Robust chaos. Phys Rev Lett 1998;80:3049–52. doi:10.1103/PhysRevLett.80.3049.
[14] Banerjee S, Grebogi C. Border-collision bifurcations in two-dimensional piecewise smooth maps. Physical Review E 1999;59(4):4052–61. doi:10.1103/PhysRevLett.80.3049.
[15] Glendinning P, Wong C. Two-dimensional attractors in the border-collision normal form. Nonlinearity 2011;24:995–1010. doi:10.1142/s0218127419300416.
[16] Glendinning P. Bifurcation from stable fixed point to two-dimensional attractor in the border collision normal form. IMA J Appl Math 2016;81(699). doi:10.1093/imamat/hxw001. –
[17] Simpson DJW, Meiss JD. Neimark–sacker bifurcations in planar, piecewise-smooth, continuous maps. SIAM J Appl Dyn Syst 2018;7:795–824.
[18] Sushko I, Gardini L. Center bifurcation for two-dimensional border-collision normal form. Int J Bifurcation and Chaos 2008;18(4):1029–50.
[19] Sushko I, Gardini L. Degenerate bifurcations and border collisions in piecewise smooth 1d and 2d maps. Int J Bifurcation and Chaos 2010;20:2045–70.
[20] Sushko I, Maistrenko Y, Gardini L. On chaotic attractors at the transition from homeomorphism to endomorphism in a family of two-dimensional piece-wise linear maps. Grazer Mathematishe Berichte 1999;339:335–46.
[21] Gardini L, Tikjha W. The role of virtual fixed points and center bifurcations in a piecewise linear map. Int J Bifurcation Chaos 2019;29(14). doi:10.1142/s0218127419300416. –
[22] WTikjha, Lapierre EG, Sitthiwirattham T. The stable equilibrium of a system of piecewise linear difference equations. Adv in Diff Equations 2017;67. doi:10.1186/s13662-017-1117-2.
[23] Mira C, Gardini L, Barugola A, Cathala J. Chaotic Dynamics in Two- Dimensional Nonivertible Maps. 1. Singapore: World Scientific; 1996.